Symposium on Applied Aerodynamics and Design of Aerospace Vehicle (SAROD 2009)
December 10-12, 2009, Bangalore, India

Three-dimensional shock/turbulent boundary layer interaction in a simulated scramjet inlet

V Pawar*, N Rane[!] and K Sinha+
Indian Institute of Technology, Bombay, India.
(krish@aero.iitb.ac.in)

ABSTRACT

The interaction of shock waves generated in a scramjet inlet with the boundary layer on the walls can result in a complex flowfield. This can have important implications for the performance of the inlet. Understanding the flow physics and predicting them reliably is a challenging task. In the current paper, the three-dimensional flowfield generated by the interaction of the cowl shock with the boundary layers on the walls of the inlet is studied computationally. The solution is analysed in detail and a description of the flow topology is presented. The side wall boundary layer is found to separate and roll up into a large longitudinal vortex. The flow is also characterized by the formation of a complex pattern of shock waves interacting with each other. The flowfield has striking resemblance to the double-fin configuration that has been studied extensively in literature.

Key Words: oblique shock, side wall effect, boundary layer separation, longitudinal vortex, shock-shock interation

NOMENCLATURE

M_∞ = Free stream Mach number

T_∞ = Free stream temperature

P_∞ = Free Stream Pressure

N = Node

F = Focus

SP = Saddle point

S = Separation line

R = Reattachment line

SUBSCRIPTS

L = Wall-Side
R = Cowl-Side

_

*Research Assistant, Indian Institute of Technology, Bombay

[!]Post Graduate Student, Indian Institute of Technology, Bombay

+Assistant Professor , Indian Institute of Technology, Bombay

1. INTRODUCTION

The development of Hypersonic air-breathing propulsion is one of the key areas of research for today's state-of-the-art aerospace technology. In order to design and develop a hypersonic propulsion system, we need to understand the underlying physics and its implications on various performance parameters from practical point of view. In case of hypersonic inlet flows, the shock wave/boundary layer interaction (SWBLI) plays a crucial role and affects the performance substantially. A shock when interacts with boundary layer gives rise to flow separation and complex three dimensional flow structure which may not be intuitive. Flow separation is a big concern for hypersonic inlets, as it causes problems in starting, blockage to the flow, high localized heat transfer rates and results in highly non-uniform flow to the combustion chamber hampering its efficiency.

It is also important to understand the flow physics in details, so that a more efficient inlet configuration can be designed by minimizing or eliminating flow separation and its effects. Complex geometries of practical hypersonic inlets are therefore broken into fundamental pieces and studied in details to understand the phenomenon thoroughly. For this purpose, CFD is a very powerful tool when validated with experimentation, as it can provide very fine details and thorough understanding of the flow structure. With this motivation, the separation caused by the cowl shock when it interacts with the boundary layers on the side walls and the wall opposite to the cowl is carefully studied through a simplified geometry in the work presented here. Such basic configurations have been extensively studied, both experimentally and numerically, for past many years. The single and double fin configurations are most relevant to practical scramjet inlets. In the presented work, the emphasize is given on the three dimensional structure of the flow and occurrence of SWBLI.

An extensive amount of work has been done on single-fin geometry, which gives rise to a quasi-conical vortical separation region with Type IV shock-shock interaction. The detail reviews on this work can be found in Panaras [1], Settles [2], Degrez [3] and Delery [4]. Few attempts have been made to explore the three dimensional structure in double fin case. The pioneering work has been done by Gaitonde *et al.* [5], [6], [7] and [8] by study important various possible configurations (i.e. symmetric and asymmetric) using CFD. The configurations are based on the experimental work of Zheltovodov *et al.* [9]. Gaitonde *et al.* [5] have studied the symmetric case of 15x15 for Mach numbers 8.3 and 4. They propose various regimes of fluid constituting the complex interaction, namely Separated Boundary Layer (SBL), Vortex Interaction (VI), Centerline Vortex (CV) and Entrainment Flow (EF). These regimes have been identified and explanation for the observed flow features is presented with the help of flow topology. Details of the shock structure, vorticity fields and their relation to the flow structure are also presented.

In the consequent work, all possible combinations of 7, 11 and 15 deg. fins have been studied. In one of the papers [7], they have explicitly study the side-wall effects in an asymmetric case numerically and features like helical vortex in the separation bubble and corner flow attaching on the side-wall are identified. Also few notable works are done considering the effects of sidewalls on SWTBLI in a rectangular channel with shock generators and compression ramps, [10], [11]. In this literature the helical vortices are found in the separated region, near the sidewalls. The details of the configuration, the code and grid used are provided in next few sections. The following subsections describe in details the kinematics and dynamic aspects of the flowfield. Various flow regimes have been identified and explained. A detailed explanation is provided for separation region. Also the shock structure has been described in the last section.

2. CONFIGURATION

A typical scramjet inlet with cowl shock is imitated through a simplified geometry. The configuration (shown in Fig. 1(a)) consists of a duct with a 21 deg shock generator simulating the cowl. The Cowl shock interacts with incoming boundary layer on Ramp surface and Side wall. Figure 1(b) shows the nomenclature of three adjacent surfaces of the geometry, adopted for ease of explanation throughout the paper. Only half of the geometry is simulated because of symmetry about the mid-plane. The flow conditions at the inlet correspond to those obtained downstream of the ramp shocks in a realistic vehicle flying at Mach 6.5.

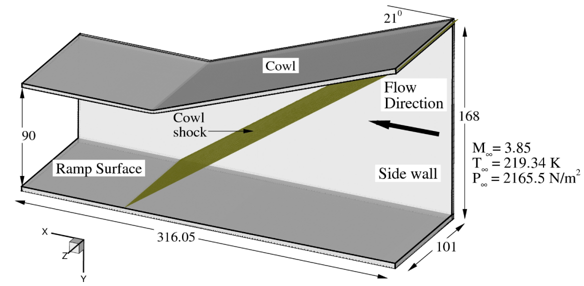

(a)

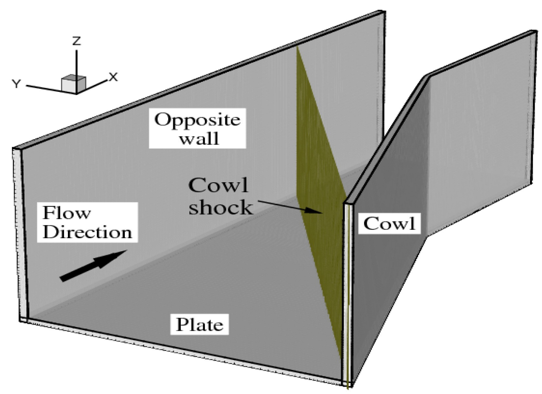

(b)

Figure 1 (a) 3D Scramjet inlet geometry.
(b) Actual nomenclature of the respective surfaces of the geometry

3. SIMULATION METHODOLOGY

We solve the Reynolds Averaged Navier-Stokes equations for the mean flow. The Spalart-Allmaras (SA) model is used for calculating the eddy viscosity. In-house code of Sinha *et al.* [12] is used in the simulations and is run on parallel machines using MPI. The governing equations are discretized in a finite-volume formulation where the inviscid fluxes are computed using a modified (low-dissipation) form of the Steger-Warming flux-splitting approach. The method is second order accurate both in stream-wise and wall normal directions. The implicit method is used to integrate in time and to reach steady-state solution. The code is validated in several high-speed flow applications. (Note: Relevant references can be found in [12]).

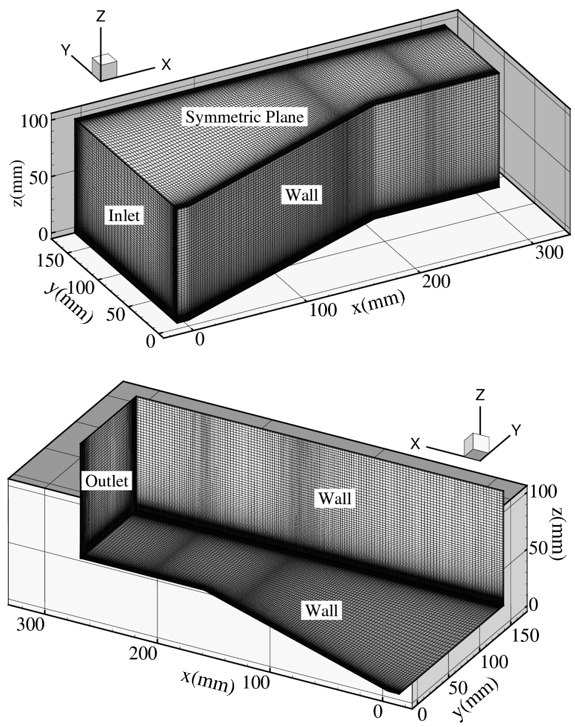

Figure 2 Proposed grid for the geometry

The computational domain and the three-dimensional grid used in the simulation are shown in Fig. 2 with two different views of orientation. Each face of the domain is labeled with their respective boundary conditions applied. The orientation of the domain is altered for convenience of analysis. There are 163 points in the streamwise (i) direction with clustering at the cowl tip and shoulder. The spanwise (j) direction between the cowl and opposite wall has 200 points. The vertical direction (k) between the bottom plate and the symmetry plane is covered by 151 points. Fine spacing is used in the near wall region on the cowl, opposite wall and the bottom plate to provide adequate resolution of the boundary layer.

Overall the single-block grid has about 5×10^6 points and is computed on 20 cpu-cores. A total of 44,000 time-steps are computed at a maximum CFL number of 500 to reach a steady-state solution. A typical simulation takes about 960 cpu-hours on a 2.66 GHz Intel processor based machine.

4. SIMULATION RESULTS

The shock structure and the three-dimensional flow pattern developed in the inlet duct are discussed in this section. Figure 3 shows the shock structure on the symmetry plane, in terms of the computed pressure gradient magnitude. The symmetry plane is located away from the plate and the flow pattern is similar to that observed in a two-dimensional reflection of an oblique shock from a boundary layer. The cowl leading edge generates the primary shock, denoted by 3_R, which interacts with the turbulent boundary layer formed on the opposite wall resulting in a large separation bubble. The separation shock 3_L formed due to the blockage caused by the separation bubble interacts with the primary shock. An induced shock 9_L and transmitted shock wave 9_R are generated from the interaction point. Shock 9_R on reflection from the free shear layer over the separation bubble results in an expansion fan. A reattachment shock 19 is formed at the downstream end of the recirculation bubble.

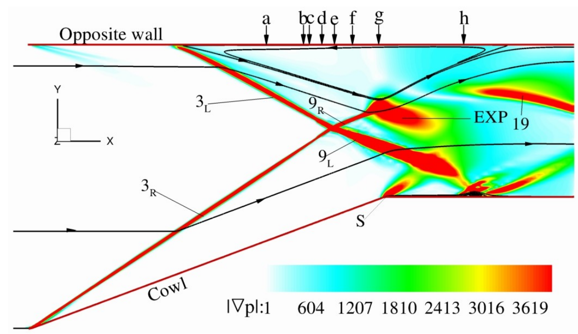

Figure 3 Shock structure at symmetric plane identified in terms of magnitude of pressure gradient

The shock pattern is similar to that presented in a crossing shock-wave/turbulent boundary layer interaction in a double fin configuration by Gaitonde *et al.* [6] and [7] . The cowl leading edge acts as one of the fins mounted on a plate. The separation bubble on the opposite wall can be taken as the other fin. However, the shape of the separation bubble changes as we approach the plate and the equivalent fin would also have a non-uniform cross-section. The nomenclature used in describing the shock pattern and the flow structure are listed in Table:1, and it matches that used in [7] closely.

The expansion fan generated by the cowl side (at point S) makes the induced shock stronger before it impinges on the boundary layer on the cowl wall. A small separation bubble is formed in the interaction region, with a shock structure similar to that of the larger recirculation bubble on the opposite wall.

The shock structure in Fig. 3 gets significantly altered in the vicinity of the plate. This is due to the three-dimensional separation of the plate boundary layer. The shock structure and the three-dimensional flow pattern are intricately related to each other. We first examine the surface streamlines on the plate and opposite wall. These lines are footprint of the three-dimensional flow and gives valuable insight into the overall flow pattern. The flowfield is also visualized in terms of various stream-surfaces that originate in different parts of the incoming flow.

Nomenclature	Description
3_R	Primary shock
3_L	Separation shock
9_R	Transmitted shock
9_L	Induced shock
EXP,13	Expansion
19	Reattachment shock
1	Primary separation shock
2	Primary Rear shock
4	Multiple Expansion-Shock reflection
6	Secondary Separation shock
7,12	Mach Stem
8	Secondary Rear shock
10	Triple point

Table 1 Nomenclature used for description of shock

Figure 4 shows the surface streamlines on the plate. Two kinds of limiting streamlines are observed. Lines of convergence, e.g. S_1 and S_2, correspond to local flow separation, and lines of divergence, like R_1 and R_2, indicate flow attaching to the wall. The streamline pattern on the cowl side is similar to that seen in a single-fin configuration, where the cowl shock causes boundary layer separation on the plate resulting in a conical region of separated flow between S_1 and R_1. A similar streamline pattern, with its separation line S_2 and attachment line R_2, originates at the separation shock on the opposite wall. The two separation lines S_1 and S_2 merge at N_1 and form the separation line S_{12} downstream. Additional separation line S_4 and an attachment line R_4 are also formed in the vicinity of S_{12}, which sand-wich a small secondary separation vortex between them. This small vortex has rotation opposite to the rotation of primary conical vortex from cowl side The line S_{12} ceases to be a separation line after some distance downstream of SP_1. Infact, the flow, attaching at R_2 can go across S_{12} in the vicinity of N_2. Nevertheless, S_{12} remains distinguishable and becomes a reattachment line R_5 downstream. Similarly, S_4 loses its prominence downstream, and it goes on to mingle with another distinct separation line S_5. A secondary vortex is formed between S_5 and R_5, which is very similar to the one formed between S_4 and R_4. Also, a very small pair of vortices (rotating in same direction) is formed on wall-side of S_5, where it starts appearing. The lines S_{12}, R_5, S_4 and S_5 mark the boundaries of Secondary Separation Region as explained later. The flow in this region comes from both, cowl-side as well as the wall-side of the domain. This feature will be explained later in the kinematical aspect of the flow.

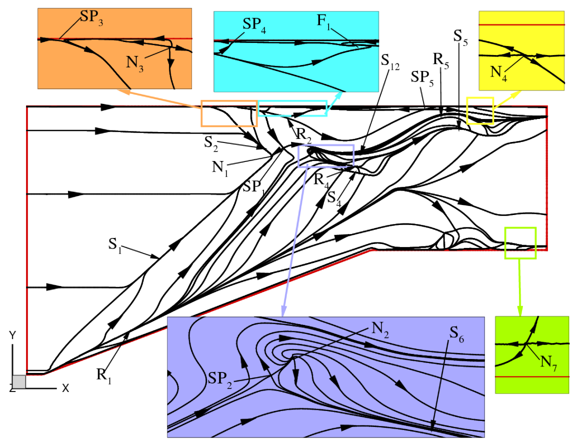

Figure 4 Surface stream lines plotted on bottom plate, along with critical points

Along with this, several critical points are also identified on the plate, which characterize the flow near the boundary. The shear stress is zero at these points and they are qualified in terms of the streamlines in their vicinity. For example, point N_1 at the intersection of separation lines S_1 and S_2 is a node of convergence and signifies flow separation. On the other hand, node point N_2 (see inset in Fig. 4) is a point of divergence and represents local flow attachment. Saddle points SP_1, SP_2, etc. have streamlines approaching along two directions and leaving along two other directions. These points demarcate flows coming from different regions and do not allow them to mix with each other. Several other critical points are identified in Fig. 4. These points follow the well known topological rule mentioned by Tobak and Peake [13].

Gaitonde *et al.* [5] has described a diamond-like structure, characterized by two nodes and two saddle points, forming at the centerline for the 15x15 deg symmetrical case. It seems N_1, SP_1, N_2 and SP_2 correspond to this diamond-like structure, although N_2 and SP_2 are blown towards the weaker side, distorting the flow topology. Also, whether the secondary vortex forming between S_4 and R_4 is related to the centerline vortices mentioned in above reference, is matter of future research.

A number of critical points are identified in the corner region. These points direct the complex flow structure near the plate-wall junction and are essential in understanding it. The enlarged boxes in Fig. 4 shows all the points in this region and are explained in following subsection. An interesting point to be noted here is the streamline pattern formed at the small separation zone on the cowl, just downstream of the expansion corner exactly matches with that on the large separation zone on the opposite wall. All the critical points also match and can be co-related with each other. It can be concluded from this fact that the flow structure in case of both the separation bubbles would be very similar. So it is enough to study one of them in details.

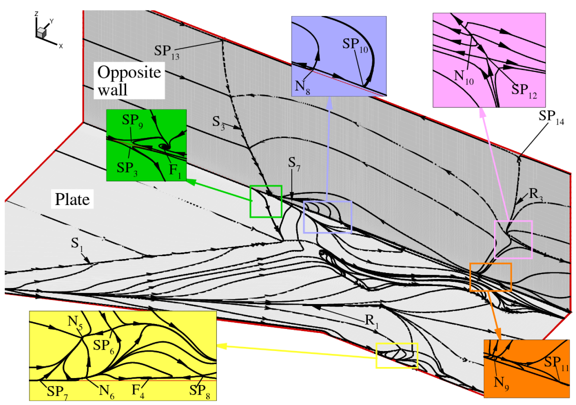

Figure 5 Surface stream lines plotted on bottom plate and opposite wall along with critical points

Figure 5 shows the surface streamlines on the opposite wall. Similar to the plate, the parallel lines corresponds to undisturbed boundary layer that develops on the wall. It separates at S_3, which is also the location where the separation shock 3_L is generated. There is an attachment line R_3, which marks the downstream extent of the separation region. The intersection of S_3 and R_3 with the symmetry plane are identified as saddle points SP_{13} and SP_{14}. These appear as the separation and reattachment points in Fig. 3. The flow pattern near the junction of the wall and the plate is characterized by additional saddle points, SP_9 and SP_{10}, and nodes of attachment, N_8 and N_9 (see inset in Fig. 5). SP_{12} separates the flow originating from N_9 and N_{10}, which is attaching on the wall, downstream as well as upstream of R_3. Further, a focal point F_1 appears near the junction, from which originates the line S_3. One more focus F_2 forms 0.6mm away from the wall, in the vicinity of F_1 (see inset in Fig. 10). These two foci have an important implication for the three-dimensional flow near the wall as discussed below.

4.1 Kinematic aspects of the flow

Gaitonde *et al.* [5] study the kinematics of the flow field generated by a double-fin configuration and identify various regimes in the three-dimensional separated flow near the plate. Similar flow regimes are identified in the current flow field in Figs. 6 and 8 in terms of stream surfaces. A detailed explanation of this flow regimes is given below.

Whole of the incoming boundary layer separates at the lines of primary separation S_1 and S_2. The fluid in the immediate vicinity of the plate (SBL) has lowest kinetic energy and thus it cannot negotiate the pressure gradient posed by the cowl shock. It tends to drift along the shock as it separates. The tendency of drifting decreases as we go away from the plate, where the fluid has more energy and is capable of negotiating the pressure gradient to an increasing extent. This is why the layers originating farther away from plate go on to attach farther downstream, and the successive layers can curl over and envelope the drifting layers below them. This results in the helical vortex structure typical of single fin configuration [16]. The incoming flow can be broken down into various regimes depending on the kind of role they play in the interaction, as proposed by Gaitonde *et al.* [5].

Separated Boundary layer (SBL): The incoming boundary layer, which is in the immediate vicinity of the plate, extending right from the cowl to the opposite wall gets separated at the separation lines S_1 and S_2 and gets drifted along them, away from the side boundaries. It never reattaches again downstream of the domain but goes on to form a part of the uplifted longitudinal vortex. It has a comparatively smaller width downstream, due to higher sweep angle of the particles near the fin leading edge. In Fig. 6 SBL is represented by blue color. It is interesting to note that a part of SBL just near the cowl-tip forms the core of the vortical structure as shown in Fig. 6 by orange colored stream-surface. Note that only a certain portion of SBL is plotted in the figure for convenience.

Vortex Interaction (VI): The layer (represented by yellow strip in Fig. 6 and 8) originates just above the SBL in the region near the cowl-tip, curls over the drifting SBL, bents down and attaches along the reattachment line R_1 in the vicinity of cowl leading edge. The fluid, after attachment, fills the gap created by SBL along the plate, flows spanwise and separates at separation line S_1 from the downstream side of it all the way till SP_1, which marks the boundary of VI. Thus it forms a shear layer with SBL. As seen in the Fig. 8, the two VI's from each side of secondary separation line S_{12}, exhibits a vortex interaction at node N_1.

Secondary vortex (SV): A narrow layer just above VI, follows a trajectory same as VI, and a part of it (represented by red strip in Fig. 6) undergoes secondary separation and forms a small helical vortex between the lines R_4 and S_4. The direction of rotation of this vortex is opposite to that of the primary conical vortex existing on same side of S_{12}. Remaining part of it impinges on plate to form a node of reattachment N_2 and spreads on it. All of the secondary vortex flow eventually separates along S_4 and S_5 from the wall side of it.

Entrainment flow (EF): The fluid layer (represented by green strip in Fig. 6 and 8) originating above VI, which is essentially the inviscid region of incoming flow, entrains high energy fluid into the near-plate region. It attaches to plate at R_1 downstream of VI. It fills the void created by separation of SBL and VI and goes on to separate along secondary separation lines S_4 and S_5. The fluid immediately above EF envelopes the conical separated region, attaches along R_1 and goes on the downstream side of it. This is nothing but the wall jet like structure identified in the cowl side quasi-conical interaction region.

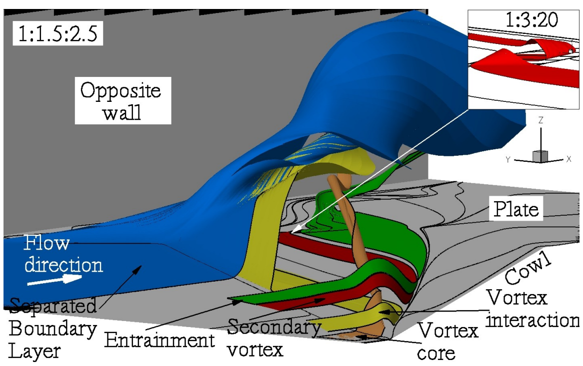

Figure 6 Multiple flow regimes identified in the incoming plate boundary layer (cowl side) indicated by streamsurfaces: Separated Boundary Layer, Vortex Interaction, Entraiment and Secondary Vortex

It is difficult to clearly differentiate these regimes from each other. The fluid which separates along downstream side of S_1 till SP_1 is VI by definition. This regime from cowl side and wall side of the domain comes together and exhibit a vortex interaction, as stated earlier. This is evident by formation of a focus (F_1') on the plane perpendicular to the plate near N_1, just above the plate (see Fig. 7). The flow which separates along secondary separation lines S_4 and S_5 is clearly EF. The void created by this separating EF is filled with flow coming from the cowl side as well as the opposite wall side. This whole fluid can be considered as Secondary Vortex (SV), similar to the Centerline Vortex (CV) described by Gaitonde *et al.* [5]. There is no clear topological boundary between SV and EF. Nevertheless, it occupies the region sandwiched between S_4, S_5, S_{12} and R_5 and shows number of small secondary separation with formation of counter-rotating vortices. As S_{12} is not distinct throughout its length, its very tricky to clearly state the boundaries of this flow on the wall-side. Towards the end of the computational domain, R_5 and S_5 combine to form a single line. Just before that, SV flow attaches at R_5 and separates along S_5 forming a counter-rotating secondary vortex similar to one formed between R_4 and S_4.

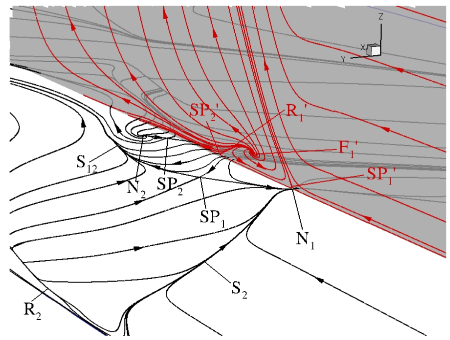

Figure 7 Surface streamlines (red) plotted on a plane normal to plate near Node N_1. Focus F_1' is formed due to VI from cowl and wall side

A conical structure similar to cowl-side is formed on the opposite-wall side with few notable differences. As the scale and intensity of this interaction is smaller than the cowl side, these regimes are also smaller and less distinct. Also the fact that the oblique shock originates because of the fin-like action of separation bubble and yet the bubble surface is not completely impermeable to fluid, like a wall, makes the flow structure there somewhat different from the cowl side. The flow attaching below the SBL does not come directly from the incoming flow as is the case with the cowl side. But it comes from the separation bubble, which in turn originates from the part boundary layer on the wall, near the junction, as shown in Fig. 8. This distinction of this flow field from the cowl side flow field is due to the imaginary fin surface i.e. the bubble surface. It is not completely impermeable to the flow across it like a solid wall. So some fluid from the separation bubble comes across this surface (near the junction only) to occupy the void below the SBL. The incoming boundary layer on the plate separates completely at S_2 and directly goes into the primary interaction vortex (Blue Ribbon in Fig. 8). There are two prominent conical vortices formed below this

SBL, similar to that on cowl side, the primary conical vortex and a corner vortex. The fluid that forms the inner part of the main vortex (S_2-R_2), originates from the flow just above the SBL at inlet and from the flow along the wall near the corner. Unlike VI and EF in the cowl-side vortex, the layers on the wall side just above the SBL curls over and bends down, but due to some other flow attaching along the plate, it cannot envelope it from behind and attach to plate. So it forms the inner part of the main vortex (between S_2-R_2) and goes to the primary interaction along with the SBL.

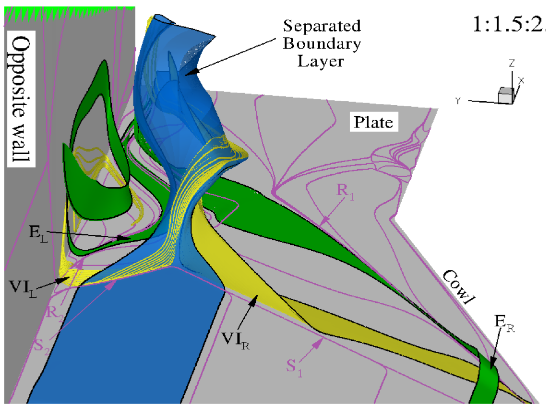

Figure 8 Flow regimes on the plate (wall side)

Similar to the flow on plate, incoming boundary layer of the opposite wall separates along S_3 constituting wall SBL. Here, the inclination of the shock 3_L with respect to the incoming boundary layer along the wall is almost negligible at symmetry plane, and goes on increasing towards the wall-plate junction and so does the tendency of fluid to drift along the shock. This is why the wall SBL (Surface 1 in Fig. 9) away from the junction just separates at S_3 without much of transverse drift, like in a 2D flow, enveloping the separation bubble below it. But as we go towards the junction, SBL (Surface 2 and 3 in Fig. 9) gets drifted towards the corner along 3_L. It goes along R_2 on the plate, but this fluid remains just above the plate, and does not attach actually to the plate. Because of this particular feature, viz. the drifting along the shock, of the SBL, only the part of it close to the junction goes in to the primary interaction happening above the plate. Rest of the SBL just envelopes the separation bubble, but it doesn't actually attach to the wall at R_3, but is separated by a thin layer of fluid whose origin is discussed later.

The interaction of the conical vortices formed on the bottom plate and the separation bubble formed on the vertical wall results in a complex flow structure in the corner region at the junction of the plate and the wall. The structure of convergence and divergence lines along with the singular points characterize the flow, divide various regimes and directs them. Figure 9 and 10 show the colored volume streamlines signifying different flow paths. The streamlines are color-coded for ease of explanation.

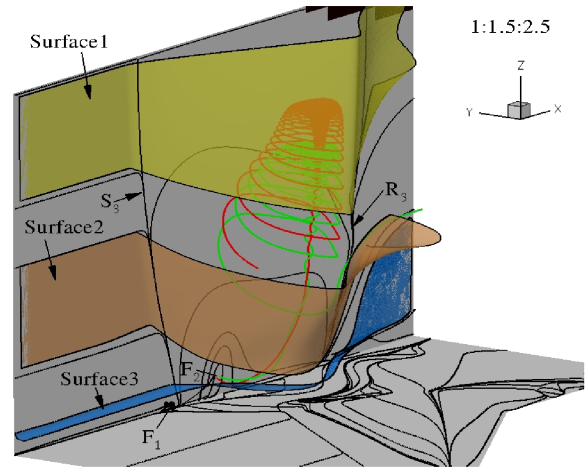

Figure 9 Structure of separation bubble on opposite wall

The fluid attaching at upstream side of R_2 and which remains in contact of plate region between S_2 and R_2 has a flow path followed by green and yellow stream lines/surfaces shown in Fig. 8 and 10. As seen from the figures this fluid has its origin from separation bubble region. The fluid initially flows along the wall and separates at S_7 (the line on wall from F_1) and part of this fluid attaches at upstream of R_2. With respect to earlier discussion of cowl side flow, this fluid co-relates to Vortex Interaction and Entrainment of wall side (yellow and green streamlines/surfaces respectively in Fig. 8).

The other part of fluid attaches on the downstream side of R_2, goes into the small corner vortex, and if it falls on upstream side of SP_4, it moves upstream towards F_1, and gets ejected through it forming the very core of the primary vortex of wallside interaction (blue streamlines in Fig. 10, inset). Otherwise the fluid goes on to converge into focus F_2, getting ejected eventually through it (Brown and maroon streamlines in Fig. 10). F_2 is formed off the surface at about 0.6mm from the wall. The vortex originating at F_2 goes towards symmetry plane, forming the core of the separation bubble. But at symmetry plane, its further movement is restricted and it unfolds onto itself forming the intermediate structure of the bubble. This is clearly shown by green and red streamlines in Fig. 9. Note that this unfolding makes the bubble to grow to a large size. Had the vortex not been restricted, the bubble would have been of a smaller size.

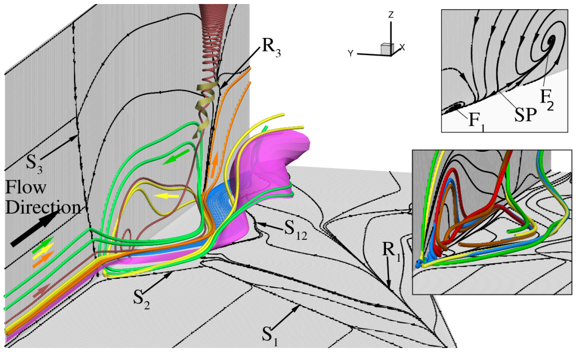

Figure 10 Structure of separation bubble at the junction of plate and wall

The incoming boundary layer along the wall, near the junction (upto 4mm from the plate), separates along the separation line between SP_3 and F_1. It goes around F_1 after separation, and envelops the vortex originating from F_1, going into the inner part of the primary conical vortex on the wall side and eventually goes in to the primary interaction above the plate. The incoming flow between the distance of 4-20mm approximately, separates along S_3. It turns towards the plate, as explained earlier, and goes along R_2 but not really attaching to the plate. R_2 marks the footprint of the separation bubble on the plate. The fluid between the region 4-5mm from the plate, curls around the primary conical vortex, forming its outer part and separates along S_{12} to go into the primary interaction (Purple ribbon in Fig. 10). Fluid originating just above this (between 5-7 mm) lingers along the plate, just above it, on the wall-side of S_{12} (Blue ribbon in Fig. 10).

The fluid between 7-9mm, goes on to attach at N_9, where it either goes into the separation bubble (see the brown, maroon and blue streamlines in Fig. 10) or it goes downstream of R_3, forming the thin layer that remains actually in contact with the wall and keeps the wall SBL from directly reattaching to the wall (see the blue ribbon in Fig. 9 and the orange colored streamlines in Fig. 10). The layers of wall SBL successively away from the plate go on to attach (above the fluid from N_9) successively away from N_9 along R_3 and either go into the bubble or go to the downstream side of R_3 attaching along the plate, and is bounded by SP_{12} from going towards the symmetry plane. Note: that only the fluid coming through N_9 remains in contact with the wall. Rest all of it remains just above this very thin layer. Also one thing is to be noted that the fluid in this part of wall SBL, nearer to the junction tends to go into the bubble and the fluid away from the junction tends to go downstream of R_3. This can probably be explained as follows: the layers nearer to the junction goes very near to the plate and thus gets retarded due to viscous effects. Whereas the layers of wall SBL away from the junction remains in the inviscid region, away from the plate, and thus not retarded as much. At R_3 there is an adverse pressure gradient due to reattachment waves. This pressure gradient cannot be overcome by the retarded layers and they tends to turn away from R_3, while the later can negotiate the gradient and continues to go ahead.

Beyond 20mm, only a very thin layer in contact with the wall, after separation goes into the interaction. After separation this part of wall SBL envelopes the bubble. But the lowest part of it mingles with the bubble flow and goes into the recirculation zone. This is possible due to the permeability of bubble surface to fluid, unlike a solid wall as discussed earlier. The rest of the wall SBL just lands on the downstreamside of R_3 and lingers along the wall, separated by a thin layer of fluid from the wall. Similar to the mingling of the wall SBL fluid with recirculating fluid, some of bubble fluid also gets mixed with the wall SBL and comes out of the bubble. The above mentioned thin layer is formed due to the fluid from the bubble attaching at R_3, right from N_9 to the symmetry plane. This provides another path of escape for the trapped fluid inside the bubble. The saddle point SP_{12} separates the flow coming in direct contact with the wall, from N_9 and N_{10} respectively.

4.2 Dynamic aspects of the flow

Figure 11 shows the contours of pressure gradient in the direction of velocity ($\nabla p.U$) on cross sections at locations (a)-(h) as indicated in Fig. 3. This interaction is very closely associated with the flow structure. Note that most of these shock interactions are three-dimensional and thus cannot be shown clearly in just the cross-planes. One needs to take a careful look of the 3D flowfield to understand them clearly. Thus, only the important features are described in this section. The two conical vortices from both the sides come together and form a single large vortex. The cowl shock 3_R produces typical single fin interaction in the form of a quasi-conical flow structure on the plate boundary. This is evident by the surface streamline pattern and the shock structure present in that region. As seen in Fig. 11(a), the incoming boundary layer separates along S_1, due to the adverse gradient of 3_R. This gives rise to the separation shock 1_R. A conical recirculation vortex is created between S_1 and R_1. The reattaching VI and EF forms high speed jet-like flow which forms a shear layer on top of the separation bubble. The separation shock intersects 3_R and gives rise to the rear shock 2_R (Edney type IV interaction). A slip line is formed through this triple point. Shock 2_R reflects back and forth as a series of compression and expansion fans

4_R and 4_L between the slip line and the shear layer. The shock structure comprising of 1_R, 2_R and 3_R looks like an inverted lambda and is thus known as the Lambda-structure. Also regions of weak expansion and compressions is seen in the conical vortical structure near the plate, which explains the curvature of surface streamlines on the plate between S_1 and R_1. This quasi-conical single fin interaction is very well studied and the work is reviewed extensively by Panaras [1] and [14], Settles [2] and Degrez [3].

Similar lambda-shock structure is formed due to shock 3_L with 1_L and 2_L on the wall-side, but its scale is much smaller. The shock 3_L is curved and three-dimensional. One more fact can be noted that downstream of section in Fig. 11(b), the rear shock (2_L) starts getting weaker and disappears eventually. As we go downstream, the two above mentioned lambda structures grow in size, come closer and interact with each other in a complex manner to give rise to secondary shocks.

As the two lambda structures come closer, 1_R and 1_L intersect each other and undergo Mach reflection, forming Mach stem shock (7) (see Fig. 11(b) and (c)). 1_R is reflected as 6_L and 1_L as 6_R. Both the shocks are curved, quite weak but have strong spots near the Mach stem 7 and the plate. 6_R is highly curved near the plate, and its foot corresponds to the separation line S_{12} and a broad region on its wall-side. Similarly, the foot of shock 6_L corresponds to the turning of flow on the cowl side vicinity of SP_1 . This turning can be observed by curviness of surface streamlines plotted on cowl side and approaching towards SP_1 (see Fig. 4). As we move downstream, 1_R and 1_L moves closer and thus shock 7 moves upwards, till a point at which 1_R reaches at the junction of 3_L and 1_L (see Fig. 11(d)). Beyond this point 1_R interacts with 3_L directly, first through Mach reflection and then regular refraction as we move downstream and gives rise to 9_L. As we go downstream, 9_L continues on the same trail of 6_L and with the small separation line (not shown). Further downstream 9_L traces separation line S_4 (see Fig. 11(e)). A small reattachment shock corresponding to R_4 and separation shock corresponding to initial part of S_5 can be seen at the foot of shock 9_L (see Fig 11(f) and (g)). In the inviscid region turning of flow in streamwise direction is manifested by the shocks 3_R and 3_L.

In section (f), the shock 1_R has crossed completely. Beyond this point, the secondary shocks, 9_L and 9_R interact with each other forming a Mach stem 12 (see Fig. 11(g)). The two primary structures have completely crossed each other giving rise to secondary shock systems. The cowl-side lambda-structure (3_R,1_R,2_R) retains its shape after cross over, whereas the wall-side one (3_L,1_L,2_L) is long disappeared, which is expected in such highly asymmetric cases.

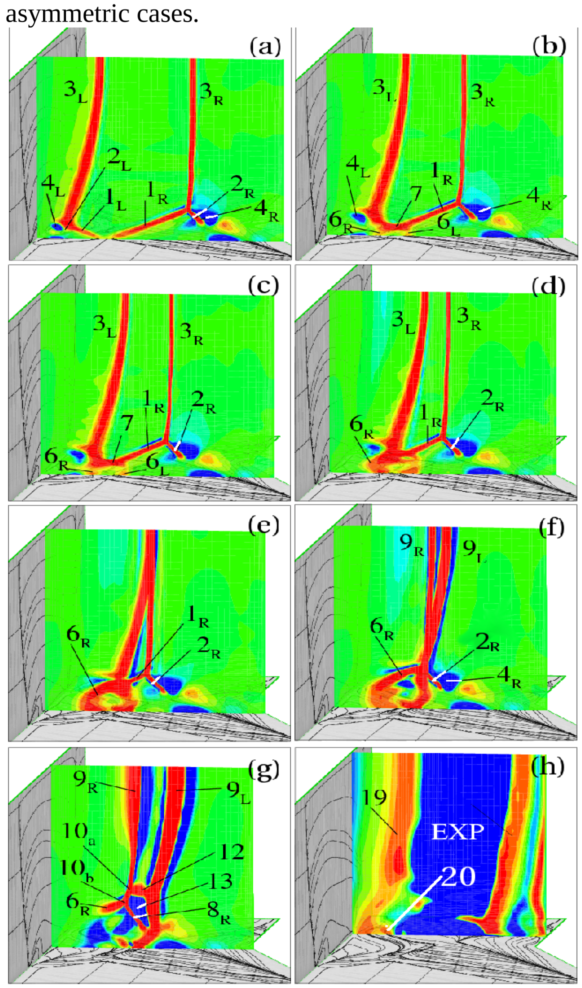

Figure 11 Shock structure at selected cutting planes plotted using ∇p.U

The secondary lambda structure on the wall-side shows 2 triple points, namely, 10_a and 10_b. Below 12, there lies an expansion fan (13), which arises due to the reflection of a part of 9_L from the shear layer of wall-side lambda structure. This is a 3D interaction and cannot be seen on the sections shown. This expansion is projected in streamwise direction towards the exit and thus can be seen in the cross-sections in Fig. 11(h). As we move ahead, the secondary lambda structure (9_R,6_R,8_R) reflects as an expansion fan from the shear layer formed on top of the wall-side separation bubble and disappears eventually. Further downstream, reattachment shock (19) shows up along with a small separation shock (20) corresponding to S_5 (see Fig. 11(h)). The shock 19 is formed due to the turning of flow to align itself to the wall. Shock 19, along with shocks 3 and 9 make the flow negotiate the separation zone and realign itself to the streamwise direction. The shock 9_L, after interaction with the cowl shoulder expansion fan, bends slightly and hit on the cowl wall giving rise to new shock wave/boundary layer interaction similar to the that formed on the wall. This forms the tertiary system of shocks on the wall side, which, except the scale, is almost similar to the one on the wall-side.

5. CONCLUSION

The shock wave/turbulent boundary layer interaction caused by the cowl shock in a typical scramjet inlet is simulated using a simplified geometry. The reflection of the cowl shock from the opposite wall is studied with special attention to the three-dimensional effects caused by the presence of the side wall boundary layer. The computed flowfield is analysed in terms of the surface streamline pattern, three-dimensional flow topology and the shock structure in a series of cross-sectional planes. The side wall boundary layer separates due to the cowl shock and the shock generated by flow separation on the opposite wall. It rolls up into a large longitudinal vortex. Additional vortices are formed in the vicinity of the wall due to secondary separation. The lambda-shock structures formed on the cowl side and the opposite wall intersect to form a complex pattern of Mach stems and triple points. The overall flow pattern on the side wall is similar to that observed in an asymmetric double fin configuration, for which experimental and numerical results exist in literature.

Acknowledgment

We would like to thank Indian Space Research Organization (ISRO) for supporting this research under the RESPOND program.

REFERENCES

(1) A. G. Panaras, "Review of the Physics of Swept-Shock/Boundary Layer Interactions," Progress in Aerospace Sciences, Vol.32, 1996.

(2) G. S. Settles, "Shock-Wave/Boundary Layer Interactions in Supersonic and Hypersonic Flows," AGARD Report, No.792, Chap.1, May 1993.

(3) G. Degrez, "Shock-Wave/Boundary Layer Interactions in Supersonic and Hypersonic Flows," AGARD Report, No.792, Chap. 2, May 1993.

(4) J. M. Delery and A. G. Panaras, "Shock Wave/Boundary Layer Interactions in High-Mach-Number-Flows," AGARD Report, Vol.2, No. 319, Chap. 2, 1996.

(5) D. V. Gaitonde, J. S. Shang, and M. Visbal, "Structure of a Double-Fin Turbulent Interaction at High Speed," AIAA Journal, Vol.33, No.2, February 1995.

(6) D. V. Gaitonde and J. S. Shang, "Structure of a Turbulent Double-Fin Interaction at Mach 4," AIAA Journal, Vol.33, No.12, December 1995.

(7) D. V. Gaitonde, M. R. Visbal and J. S. Shang, "Sidewall Interaction in an Asymmetric Simulated Inlet Configuration," Journal of Propulsion and Power, Vol.17, No.3, May-June 2001.

(8) D. V. Gaitonde, J. S. Shang, T. J. Garrison, A. A. Zheltovodov and A. I. Maksimov, "Three-Dimensional Turbulent Interactions Caused by Asymmetric Crossing-Shock Configurations," AIAA Journal, Vol.37, N0.12, December 1999.

(9) A. A Zheltovodov, A. I. Maksimov, A. M. Shevchenko and D. D. Knight, "Topology of Three-Dimensional Separation under the conditions of Asymmetrical Interaction of Crossing Shock and Expansion waves with Turbulent Boundary Layer," Thermophysics and Aeromechanics, Vol.5, No.4, 1998.

(10) V. I. Kornilov, "Correlation of the separation region length in shock wave/channel boundary layer interaction," Experinments in Fluids, 1997.

(11) J. Dussauge, P. Dupont and J. Debieve, "Unsteadiness in shock wave boundary layer interactions with separation," Aerospace Science and Technology, Vol.10, 2006.

(12) K. Sinha and G. V. Candler, "Convergence Improvement of Two-Equation Turbulence Model Calculations," AIAA paper, 1998.

(13) M. Tobak and D. J. Peake, "Topology of Three-Dimensional Separated Flows," NASA Technical Memorandum 81294, April 1981.

(14) D. Knight, H. Yan, A. G. Panaras and A. A. Zheltovodov, "Advances in CFD prediction of shock wave turbulent boundary layer interactions," Progress in Aerospace Sciences, Vol.39, 2003.